Electroweak phase transition in the 2HDM: collider and gravitational wave complementarity

Ajay Kaladharan

With Dorival Gonçalves and Yongcheng Wu

Arxiv:2108.05356

May 9, 2022

Pheno 2022

Oklahoma State University

Collider and GW Complementarity

Probing the shape of the Higgs potential

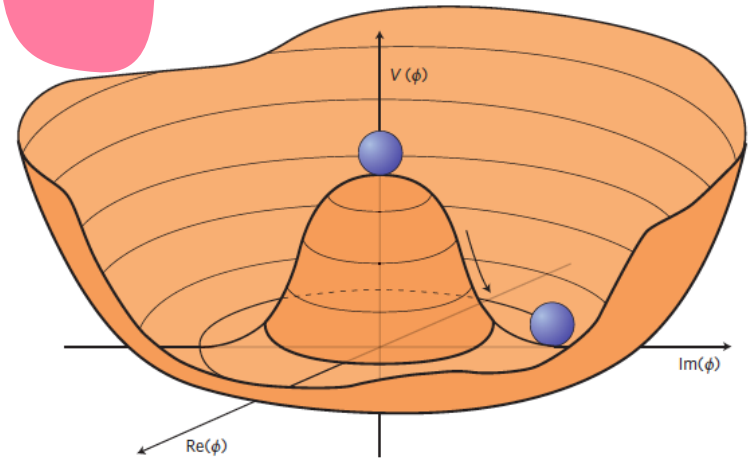

Bound on the triple Higgs-coupling are weak

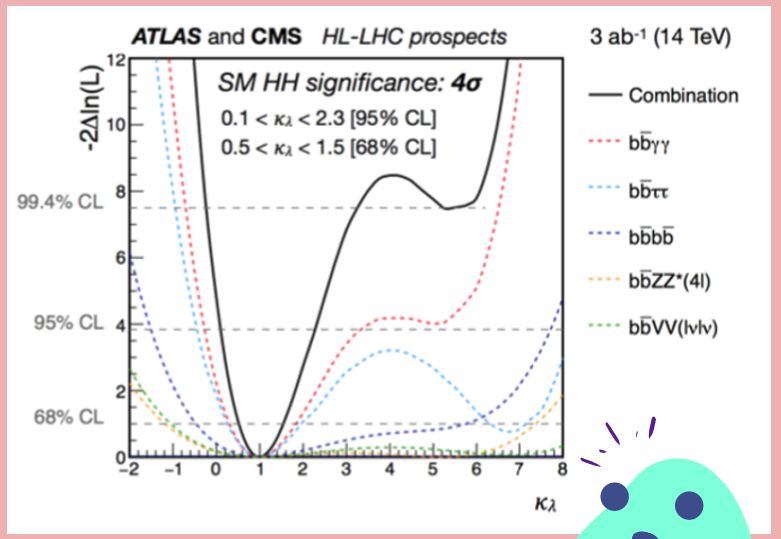

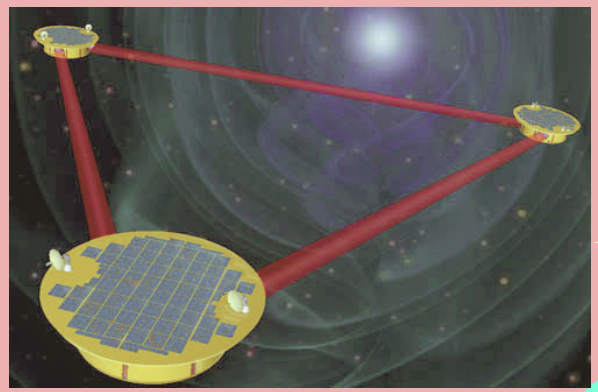

GW detector-new window

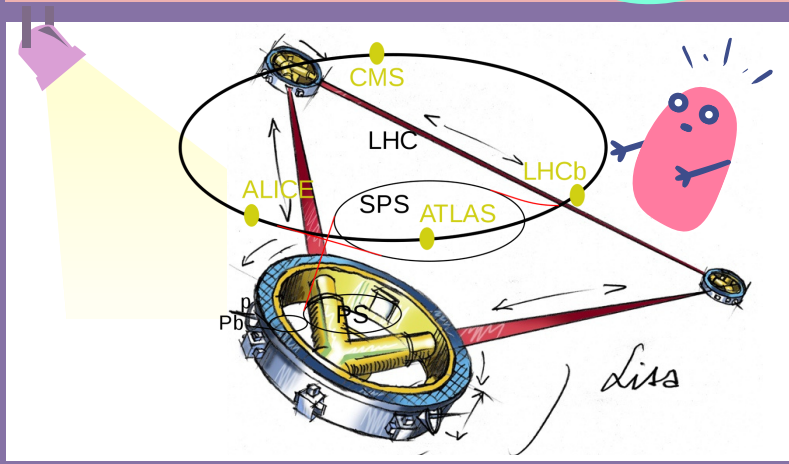

CP-conserving THDM

- CP-conserving 2HDM with a softly broken $\mathbb{Z}_2$ symmetry.

$$V(\Phi_1,\Phi_2) = m_{11}^2\Phi_1^\dagger\Phi_1 + m_{22}^2\Phi_2^\dagger\Phi_2 - m_{12}^2(\Phi_1^\dagger\Phi_2 + h.c.) + \frac{\lambda_1}{2}(\Phi_1^\dagger\Phi_1)^2$$
$$+ \frac{\lambda_2}{2}(\Phi_2^\dagger\Phi_2)^2 + \lambda_3(\Phi_1^\dagger\Phi_1)(\Phi_2^\dagger\Phi_2) + \lambda_4(\Phi_1^\dagger\Phi_2)(\Phi_2^\dagger\Phi_1) + \frac{\lambda_5}{2}\left((\Phi_1^\dagger\Phi_2)^2 + h.c.\right),$$

- $\mathbb{Z}_2$ symmetry transformations $\Phi_1 \to \Phi_1$ and $\Phi_2 \to -\Phi_2$

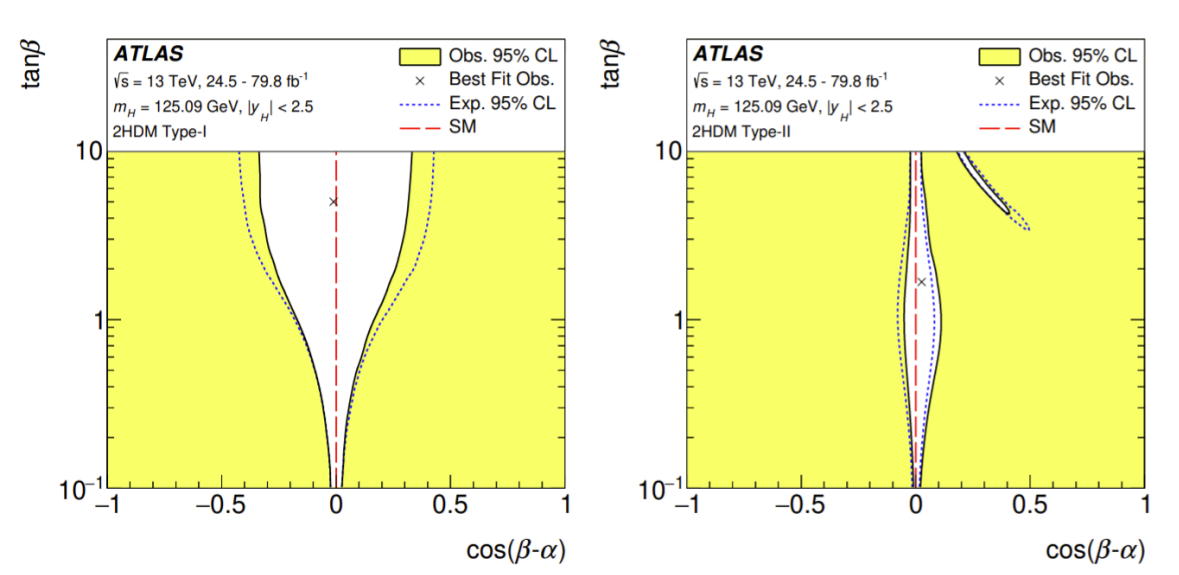

t_β-$C_{\beta-\alpha}$ plot, left side corresponds to type I and right side corresponds to type II

$$tan\beta = \frac{v_2}{v_1}$$

First order phase transition

At the critical temperature, T_C symmetry broken and unbroken vacuum are degenerate.

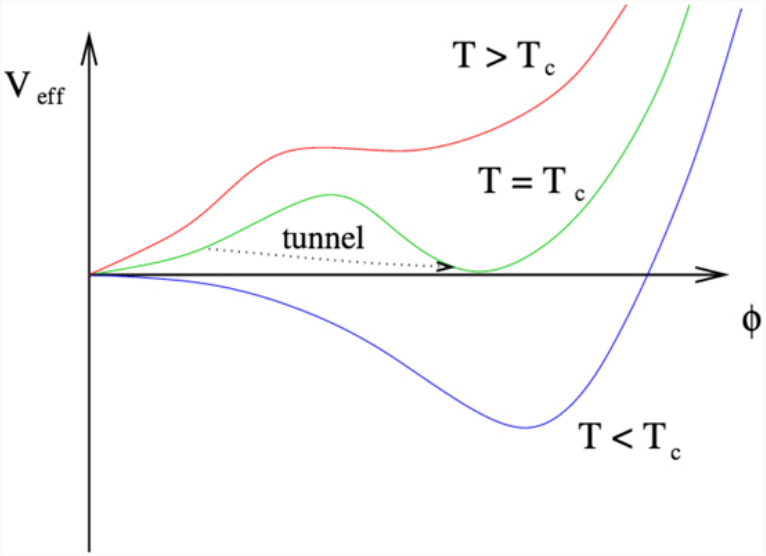

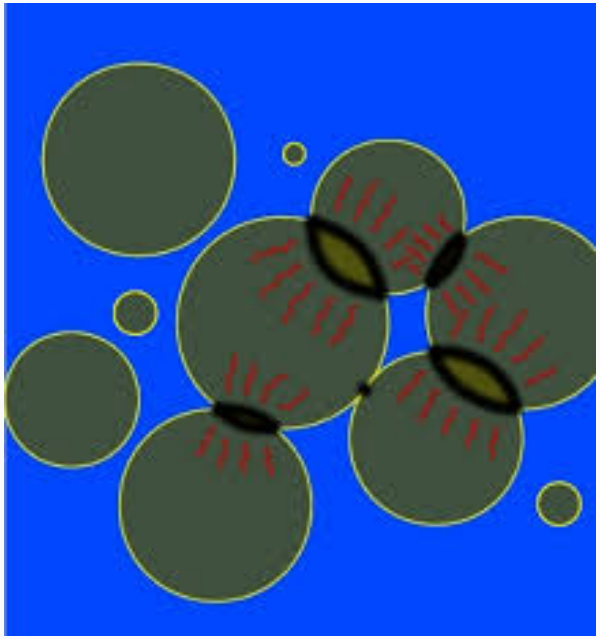

$\frac{S_3(T_n)}{T_n} \approx 140.$

$$\alpha = \frac{\rho_{vac}}{\rho_{rad}} = \frac{1}{\rho_{rad}} \left[T \frac{d\Delta V}{dT} - \Delta V \right]_{T_n}, \qquad \beta = \left(HT \frac{d(s_3/T)}{dT} \right)_{T_n}.$$

(C.Grojean, G.Servant 2007)

Electroweak phase transition

- To study the thermal evolution of the universe.
- For successful completion of electroweak baryogenesis, EWPT requires to be strongly first order, and the condition is given by,

$$\xi_c \equiv \frac{v_c}{T_c} \geq 1\,.$$

- FOPT in the early universe show detectable GW signals today.
- GW signal is detectable in detector if SNR > 10.

$$SNR = \sqrt{\tau \int_{f_{min}}^{f_{max}} df \left[\frac{\Omega_{GW}(f)h^2}{\Omega_{sens}(f)h^2}\right]^2}\,.$$

(C.Caprini et al., 2016)

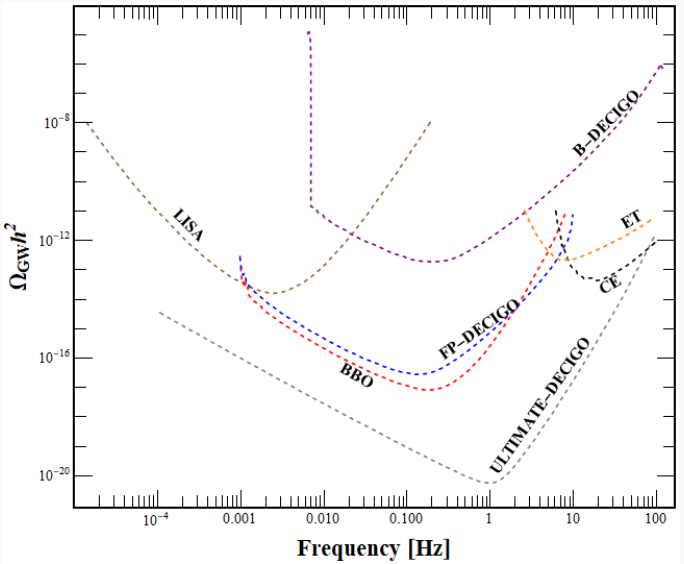

Effective potential

$$V_{\text{eff}}(\omega_1, \omega_2, T) = V_0(\omega_1, \omega_2) + V_{CW}(\omega_1, \omega_2) + V_{CT}(\omega_1, \omega_2, T) + V_T(\omega_1, \omega_2)$$
$$= V_0(\omega_1, \omega_2) + V_1(\omega_1, \omega_2) + V_T(\omega_1, \omega_2).$$

(P.B Arnold, O.Espinosa, 1993)

Shape of the potential

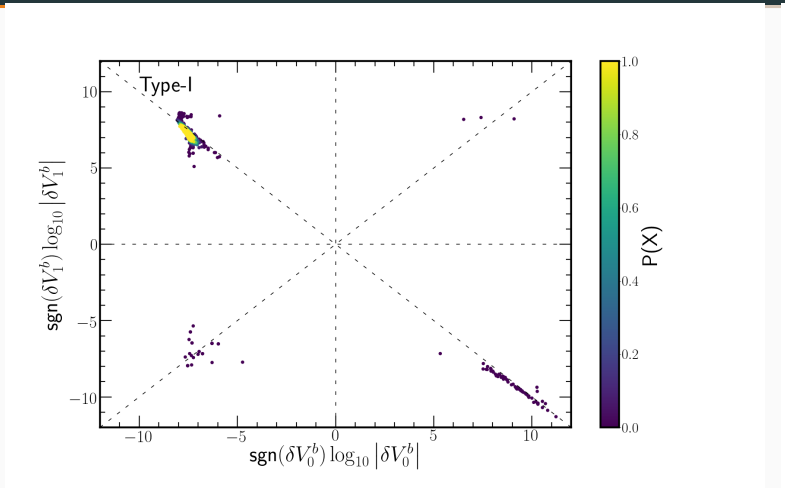

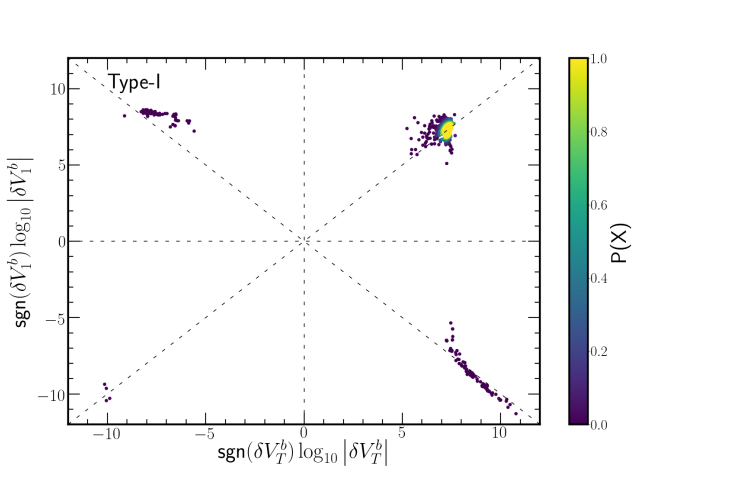

In the $\xi_c > 1$ regime, the phase transition is mostly one-loop driven.

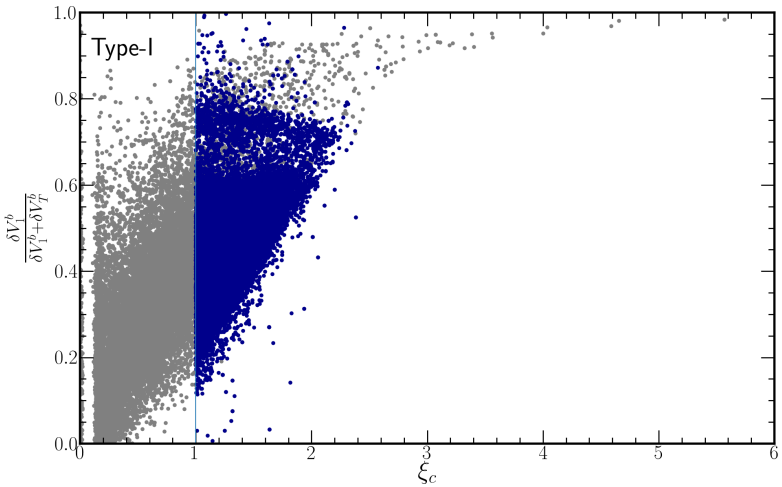

If the fraction of the barrier height provided by the one-loop contribution is close to 100%, the tunnelling from the false vacuum to the true vacuum is more challenging. For this reason, the universe with $\xi_c > 2.5$ trapped in the false vacuum.

Shape of the potential

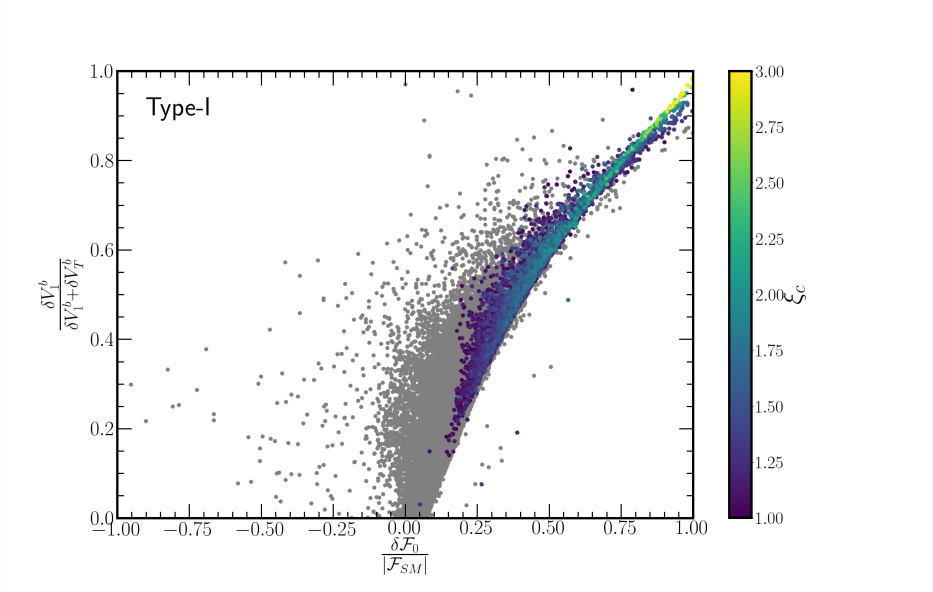

The barrier height provided by the one-loop contribution is correlated to $\Delta\mathcal{F}_0/|\mathcal{F}_0^{\rm SM}|$ which measures the vacuum upliftment at zero temperature.

$\mathcal{F}_0$ is the vacuum energy density of the 2HDM at $T = 0$ defined as

$$\mathcal{F}_0 \equiv V_{\rm eff}(v_1, v_2, T = 0) - V_{\rm eff}(0, 0, T = 0),$$

and $\mathcal{F}_0^{\rm SM} = -1.25 \times 10^8$ GeV^4.

Vacuum upliftment $\Delta\mathcal{F}_0/|\mathcal{F}_0^{\rm SM}|$

The individual contributions from H, A, and $H^\pm$ to $\mathcal{F}_0$ are of the same form.

$$\mathcal{F}_0^{1,A}(c_{\beta-\alpha}=0)=\frac{1}{512\pi^2}\left[\left(3m_h^2+2m_A^2-6\frac{m_{12}^2}{s_\beta c_\beta}\right)\left(m_h^2+\boxed{2m_A^2-2\frac{m_{12}^2}{s_\beta c_\beta}}\right)\right.$$
$$\left.+\left(m_h^2-2\frac{m_{12}^2}{s_\beta c_\beta}\right)^2\log\left(\frac{4m_A^4}{(m_h^2-2m_{12}^2/(s_\beta c_\beta))^2}\right)\right]$$

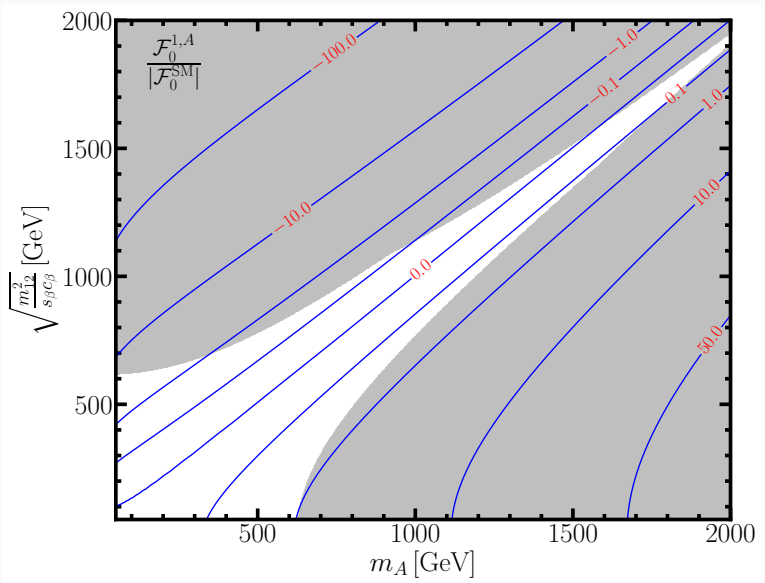

The individual contribution $\mathcal{F}_0^{1,A}/|\mathcal{F}_0^{\rm SM}|$ from A (blue solid line) in m_A-$\sqrt{m_{12}^2/(s_\beta c_\beta)}$ plane. The grey shaded region is excluded by unitarity and perturbativity constraints assuming $t_\beta=1$, $c_{\beta-\alpha}=0$, and $m_A=m_{H^\pm}=m_H+100$ GeV.

Δm_H-Δm_A

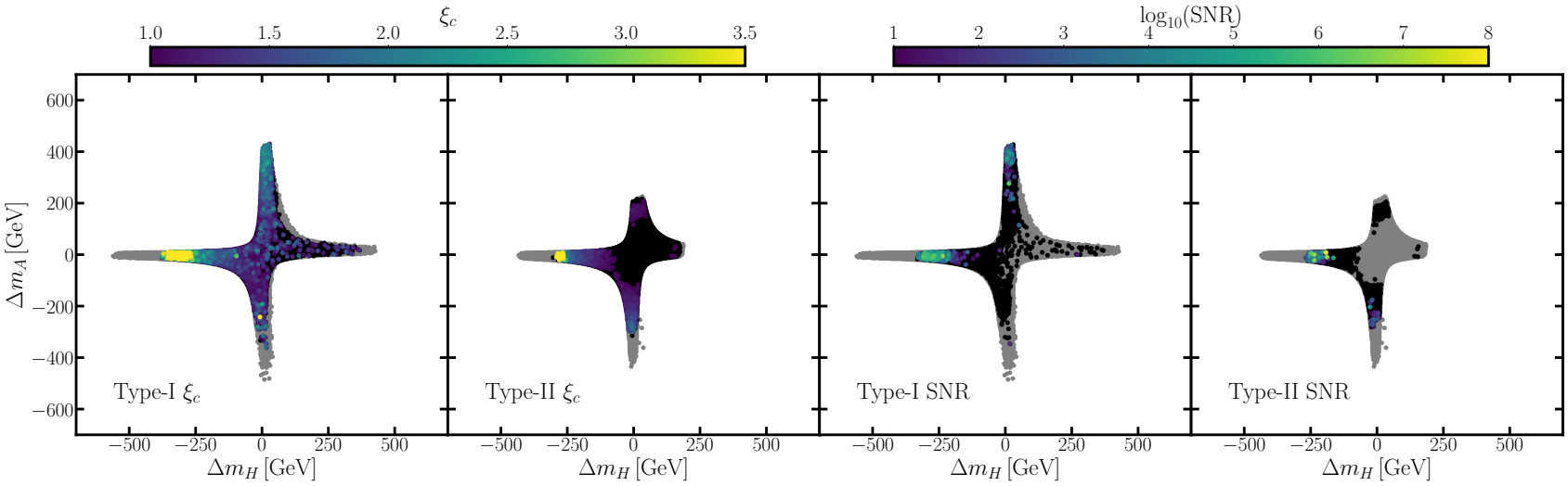

- $\Delta m_H = m_H - m_{H^\pm}$ and $\Delta m_A = m_A - m_{H^\pm}$.
- For type II, $m_{H^\pm} < 580$ GeV has been excluded by the measurements of BR($B \to X_s\gamma$).
- $m_H < m_{H^\pm} \approx m_A$ (left branch): most favourable for SFOEWPT. $m_{12}^2/(s_\beta c_\beta)$ is closer to m_H^2, this leads to large and positive contributions from A and $H^\pm$ to $\mathcal{F}_0$
- $m_H \approx m_{H^\pm} \approx m_A$ (central region): depleted number of SFOEWPT points.

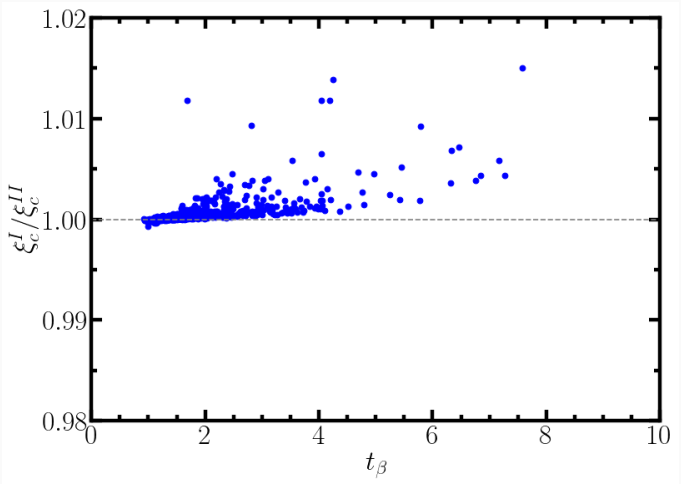

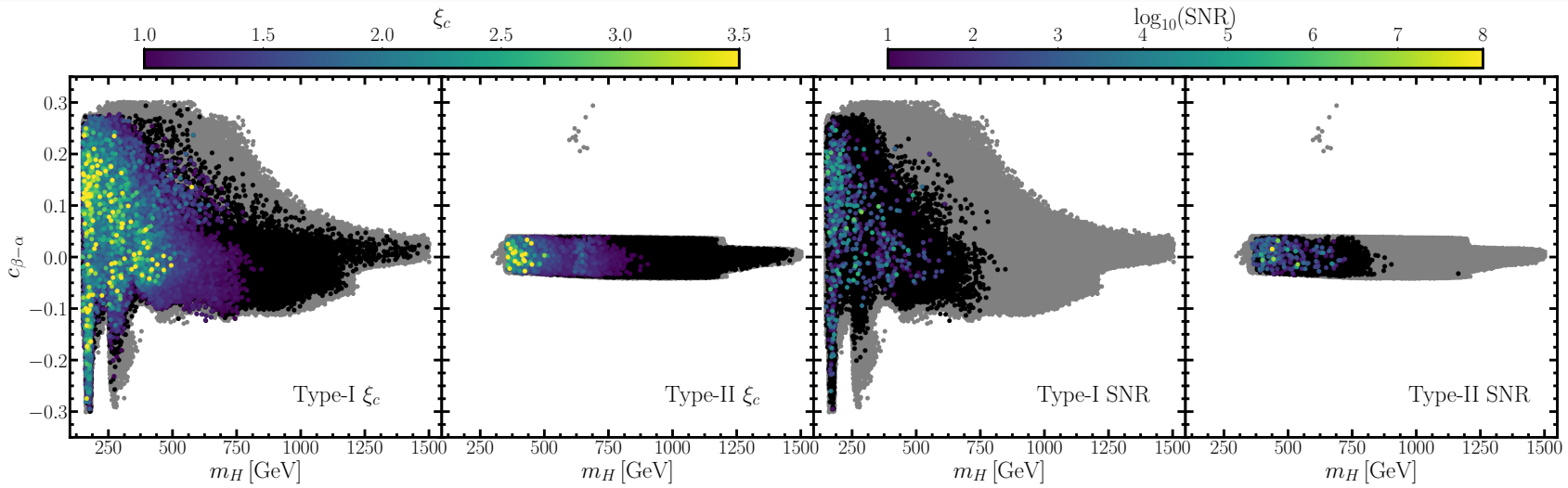

Grey: all points passing HiggsBounds and HiggsSignal. Black: all points with first order phase transition. The heat map tracks ξ_c (left) and SNR (right).

Resonant and Non-Resonant di-Higgs Searches

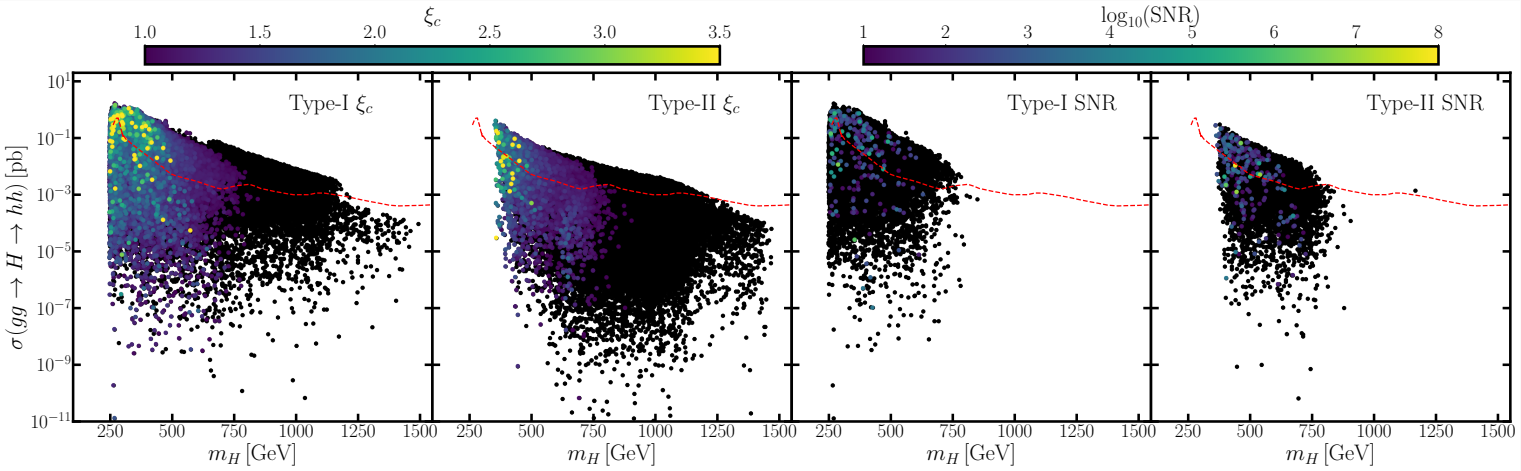

The cross section $\sigma(gg \to H) \times \mathrm{BR}(H \to hh)$ vs. m_H. The red dashed line indicates the projected limits from ATLAS with $3000\,\mathrm{fb}^{-1}$ by scaling current limits.

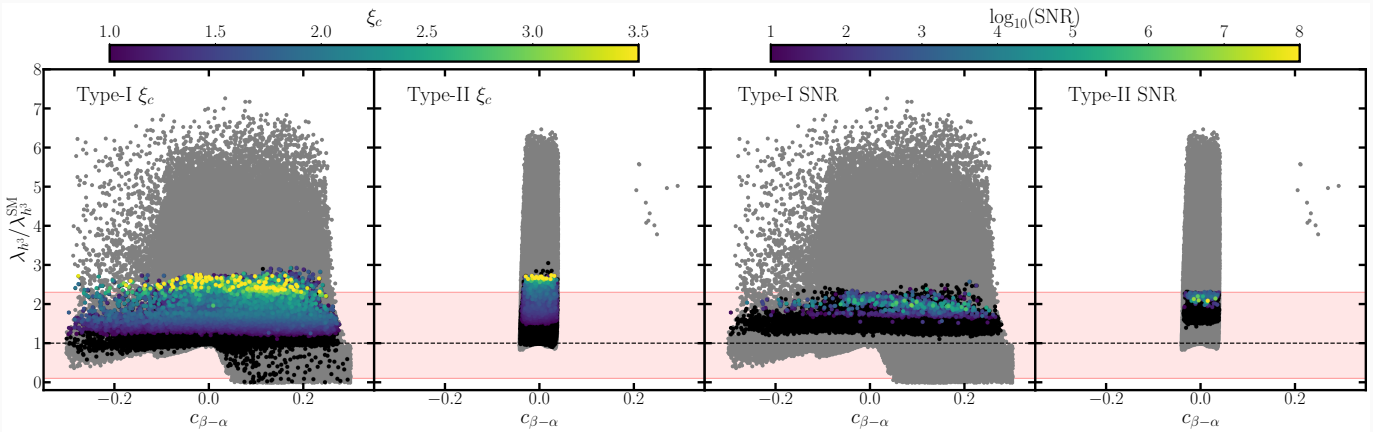

$\lambda_{h^3}/\lambda_{h^3}^{\mathrm{SM}}$ as function of $c_{\beta-\alpha}$. The HL-LHC projected 95% CL sensitivity for non-resonant di-Higgs production is also shown $0.1 < \lambda_{h^3}/\lambda_{h^3}^{\mathrm{SM}} < 2.3$ (light red)

$A \to ZH$ and $H \to ZA$ Searches

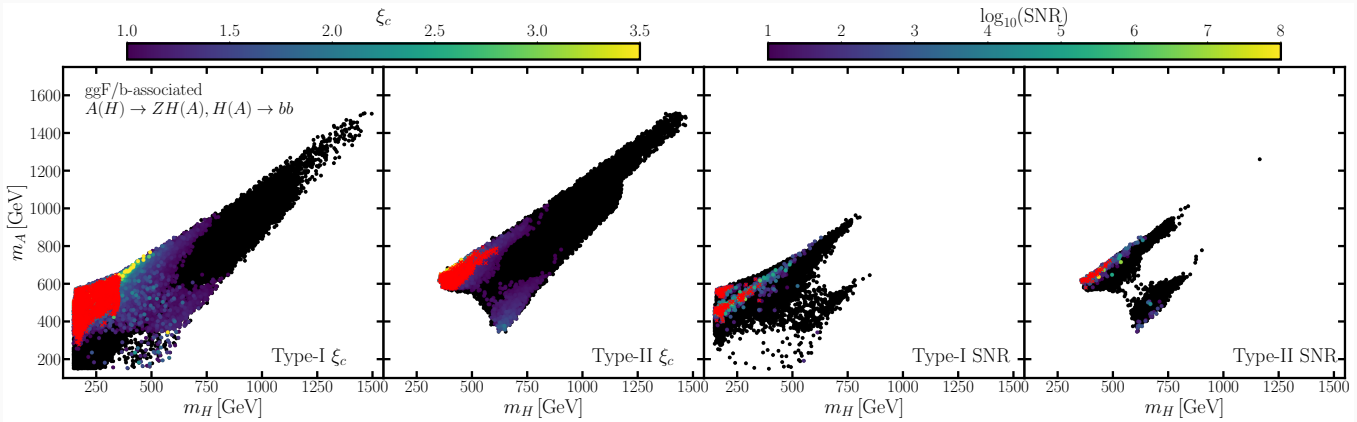

The $A \to ZH$ constraints on m_H-m_A plane. The red crosses are the points that can be probed by the HL-LHC through $A \to ZH \to \ell\ell b\bar{b}$ searches, where A is produced through gluon fusion or via b-associated production

- The widely discussed $A(H) \to ZH(A)$ channel in the context of EWPT in 2HDM is still relevant but for a smaller fraction of points compared to other searches.
- Whereas the $H \to bb$ channel generally provides the strongest limits for this channel, it quickly becomes subdominant once the scalar mass is beyond top-pair threshold.
- The $H \to WW$ channel shows smaller sensitivity as it is suppressed by $c_{\beta-\alpha}$.

Scalar Decays to Heavy Fermions

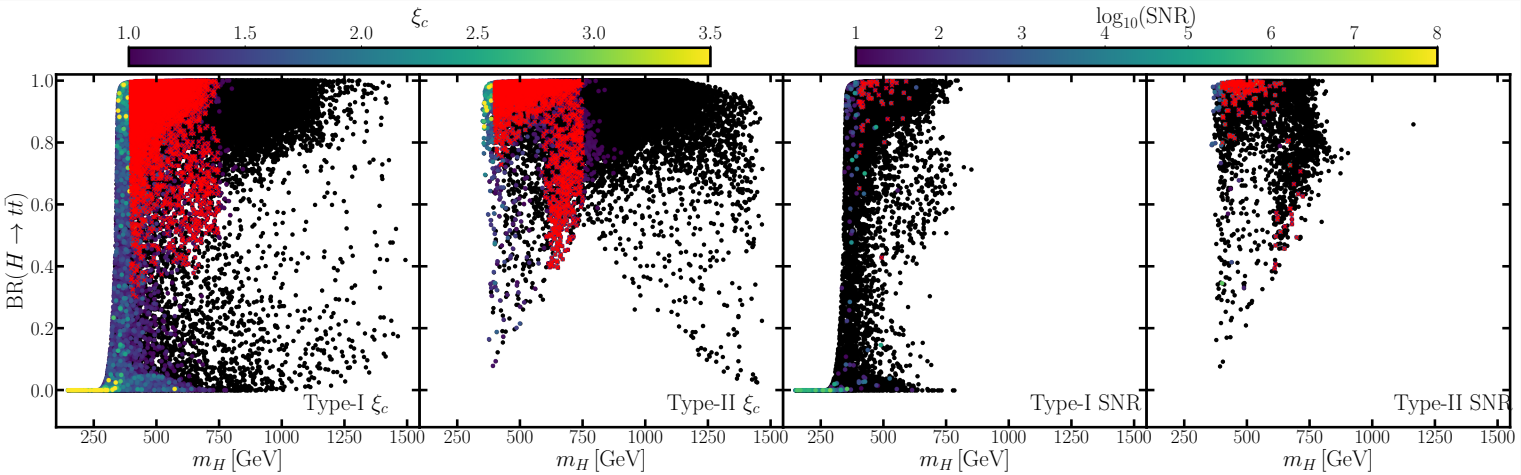

Branching fraction $\mathcal{BR}(H \to t\bar{t})$ as function of m_H. The red crosses are the points with $\xi_c > 1$ (left panels) and SNR > 10 (right panels) that can be probed by HL-LHC through resonant searches decaying to top quark pair.

- The resonant searches with heavy fermionic final states is crucial for SFOPEWPT sensitivity at the HL-LHC.
- Type-II 2HDM is more constrained at the HL-LHC for $\xi_c > 1$ points as the type-II have a stronger lower bound on scalar masses favoring the $H/A \to t\bar{t}$ search.

Combined Results

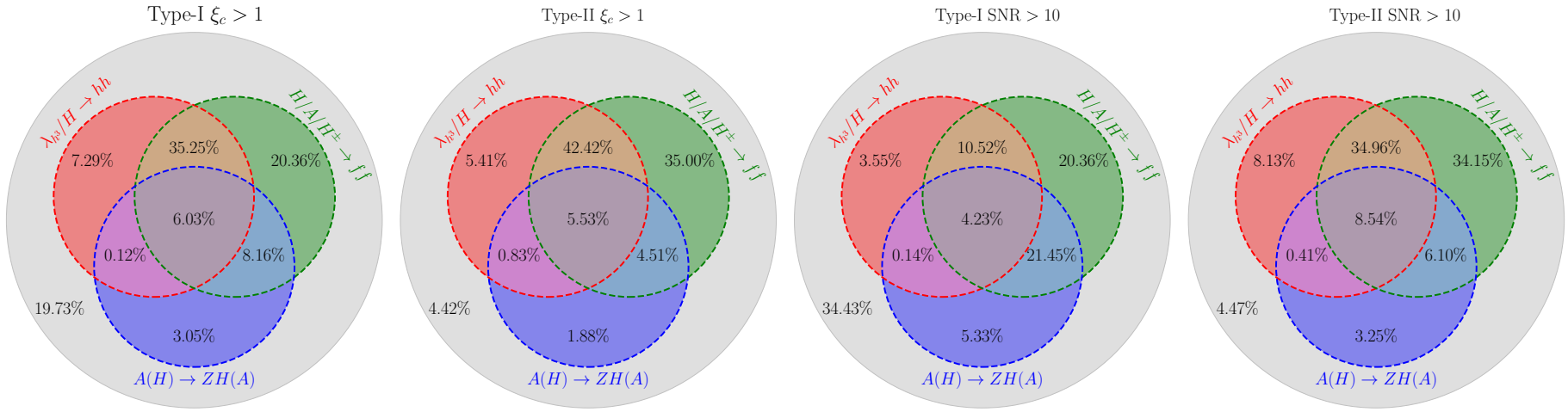

The summary of the capabilities of corresponding search channels at the HL-LHC.

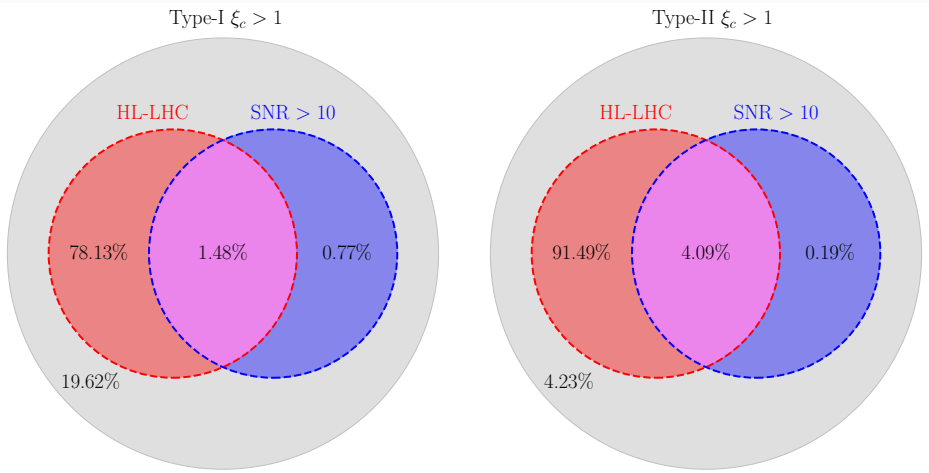

The summary of the capabilities of the HL-LHC and GW experiments.

Summary

- Type I and Type II have similar phase transition behaviour and GW signals.
- The barrier formation in the Higgs potential of the 2HDM is driven by the one-loop and thermal corrections, with the dominance of the one-loop terms for large order parameter $\xi_c > 1$
- Scalar decays to heavy fermions $H^{\pm}, H, A \to tb, tt$ is the most promising smoking gun signature for SFOEWPT at the HL-LHC, followed by the di-Higgs searches.
- In contrast to the HL-LHC, LISA is going to be sensitive to a significantly smaller parameter space region, whereas it renders to complementary sensitivities where the correspondent LHC cross-section is suppressed.

Thank you!